Vol 17 No 10, October 2008
1674-1056/2008/17(10)/3799-08

Chinese Physics B

© 2008 Chin. Phys. Soc.
and IOP Publishing Ltd

High and low frequency relaxation oscillations in a capacitive discharge plasma*

Zhou Zhu-Wen(周筑文)[a)†], Sungjin Kim[b)], Ji Shi-Yin(吉世印)[a)], Sun Guang-Yu(孙光宇)[a)], and Deng Ming-Sen(邓明森)[a)]

[a)] *Department of physics, Guizhou Educational College, Guiyang 550003, China*
[b)] *Department of Electrical Engineering and Computer Sciences - 1770 University of California, Berkeley CA 94720, U.S.A.*

(Received 14 February 2008; revised manuscript received 31 March 2008)

Both high and low frequency relaxation oscillations have been observed in an argon capacitive discharge connected to a peripheral grounded chamber through a slot with dielectric spacers. The oscillations, observed from time-varying optical emission of the main discharge chamber, show, for example, a high frequency (46 kHz) relaxation oscillation at 100 mTorr, with an absorbed power near the peripheral breakdown, and a low frequency (2.7–3.7 Hz) oscillation, at a higher absorbed power. The high frequency oscillation is found to ignite a plasma in the slot, but usually not in the periphery. The high frequency oscillation is interpreted by using an electromagnetic model of the slot impedance, combined with the circuit analysis of the system including a matching network. The model is further developed by using a parallel connection of variable peripheral capacitance to analyse the low frequency oscillation. The results obtained from the model are in agreement with the experimental observations and indicate that a variety of behaviours are dependent on the matching conditions.

Keywords: relaxation oscillation, capacitive discharge, periphery, slot
PACC: 5235, 5235P

1. Introduction

A configuration of both theoretical and practical interest is a capacitive discharge connected through a dielectric slot to a peripheral grounded region. A particular configuration, which has been found to have desirable processing applications,[1] is a dual frequency capacitive discharge, with the main cylindrical discharge connected to a peripheral cylindrical (pumping) region through an annular slot narrowed with a dielectric. The feedstock gas flows from the main discharge region through the slot, and is pumped in the grounded peripheral chamber.

In a previous study,[2] we examined both theoretically and experimentally the conditions under which the peripheral ignition occurs, and we determined the conditions required to confine the discharge to the central region.

The apparatus is illustrated in Fig.1. The discharge, having a plate separation l, is connected to a peripheral region with a width $w_{\rm per}$ through an annular dielectric slot with a gap width w and a gap spacing g. The parameters of the experiment are as follows: the radius of central discharge powered electrode $R_1 = 6.35$ cm, and the radius of the ground electrode extending to the inner radius of the dielectric slot $R_2 = 8.9$ cm, with a 2.54 cm gap between the powered electrode insulated by a quartz dielectric and the lower grounded electrode (see Fig.1). The axial separation between the powered electrode and the upper grounded electrode is $l = 2.54$ cm, the slot width is $w = 3.8$ cm, and the grounded peripheral length is $w_{\rm per}$ cm. The separation between the dielectric spacers in the slot can be varied, but in our previous study and in the experiment reported here only the widest spacing $g = 0.635$ cm is used.

An unexpected phenomenon is the observation of both high frequency (kHz range) and low frequency (Hz range) relaxation oscillations under the condition that plasma extends out of the central discharge region. Such oscillations can prevent good matching, which is one of the causes of the deterioration of the performance of reactors with peripheral breakdown. The kilohertz oscillation is initiated when a plasma is

*Project supported by the Science Foundation of the Educational Bureau of Guizhou Province in China (Grant No ECS-2006215), the Lam Research Corporation, the State of California MICRO Program, National Science Foundation (Grant No ECS-0139956), and a UC Discovery Grant from the Industry-University Cooperative Research Program (IUCRP).
†E-mail: zhuwenz@gmail.com

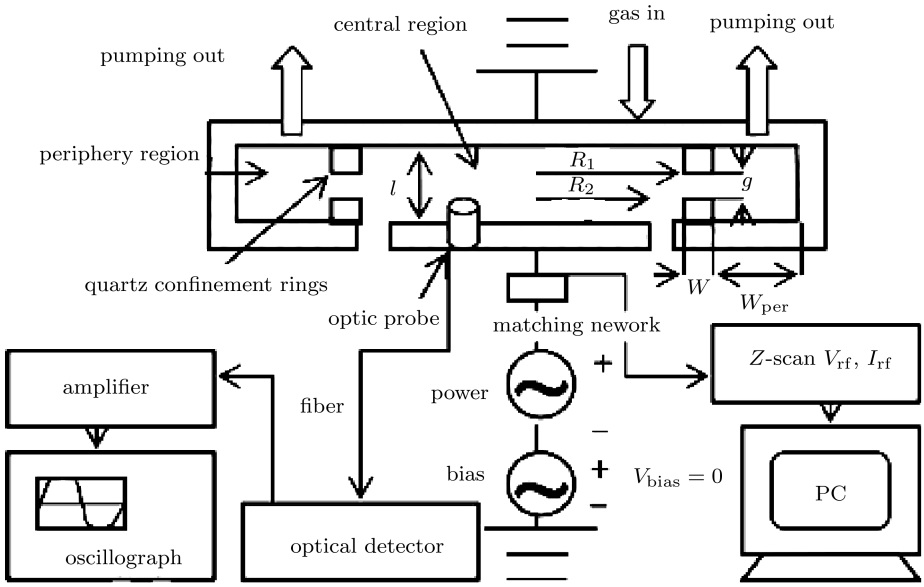


Fig.1. Schematic a capacitive discharge plasma apparatus.

ignited in the slot, but not necessarily in the periphery. The hertz oscillations occur as spatially moving plasmas, with both the slot and periphery ignited. We have observed that a hysteresis occurs such that the peripheral plasma can be maintained at a lower voltage, as shown in Fig.2, when reducing the voltage, than that required to create the peripheral discharge. Measurements are performed at 50, 75, and 100 mTorr (1 Torr = 133 Pa) in argon. For all the pressures the discharges show similar hysteresis behaviours. In this work, we present detailed measurements of the oscillations and interpret them by using an electromagnetic model of the slot impedance, combined with a circuit model of the entire system.

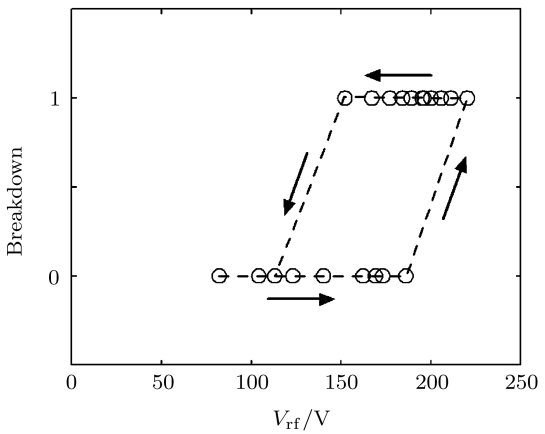


Fig.2. Hysteresis curve at 100 mTorr, with upper level indicating breakdown of peripheral plasma, and lower level indicating a confined plasma; the separation between the upper and the lower curves is only for convenience of viewing.

In Section 2, we present some typical observations of the instability. In Section 3, a theory is developed to predict the onset and the dynamics of the high and the low frequency oscillations, with the results compared with experimental observations. Conclusions and further discussion are given in Section 4.

2. Phenomenological description of relaxation oscillations

In Figs.3 and 4, the several types of relaxation oscillations that occur in the discharge are shown. The optical emission from a central region is observed through a 6 mm wide optical slot located in the ground electrode. In the figures, I is the relative optical emission intensity in the main and the peripheral discharge regions of the neutral argon emission at 748.7 nm, detected through a notch filter and a fibre optic cable. The plasma potential signal from the potential ring measurement system is also shown in Fig.3. In that figure, a high frequency relaxation oscillation (46.5 kHz) is observed at 100 mTorr and 15 W absorbed power. The peak of the plasma potential corresponds, roughly, to the peak of the light signal (the small shift is thought to be due to the instrument). The light oscillation also occurs in the slot, while, at these parameters, the periphery remains dark. In Figs.4(a), 4(b) and 4(c), at 100 mTorr and

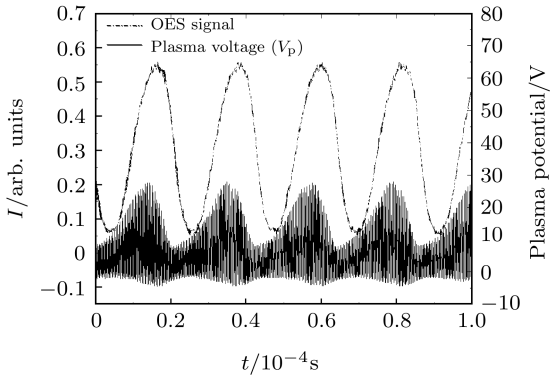


Fig.3. Time-varying optical emission I from the main discharge region, showing a high frequency (46 kHz) relaxation oscillation at 100 mTorr and 15 W absorbed power and an argon emission at 748.7 nm detected through a notch filter and a fibre optic cable, where the zero of I is not calibrated.

at 325, 260, and 176 W absorbed powers, the time-varying optical emissions from both the main and the periphery discharge show the relaxation oscillations at low frequencies (2.717, 3.484, and 3.697 Hz). The oscillation visually has spatial motion, typically balls of light rotating around the discharge. In these cases the minimum of the optical emission is close to zero, indicating that the central and peripheral discharge electrons producing the emission are cooled or absent.

In the rest of this section, and in the analysis to follow, we consider the high frequency (kilohertz) and the low frequency (hertz) oscillations. We observe the kilohertz oscillation under a variety of conditions, with the general characteristic that the behaviour corresponds to a matching network that is of somewhat mismatching at the initiation and during the oscillation. For the particular case shown in Fig.3, approximately 3/4 of the incident power is reflected just before the initiation of the oscillation. During the oscillation, the matching further degrades, with $P_{\mathrm{fwd}} = 100\,\mathrm{W}$ and $P_{\mathrm{refl}} = 85\,\mathrm{W}$, leading to the net power indicated above. In a second, somewhat higher absorbed power case, at $p = 100\,\mathrm{mTorr}$ and $P_{\mathrm{abs}} = 20\,\mathrm{W}$, the average forward and reflected powers during the instability are $P_{\mathrm{fwd}} = 100\,\mathrm{W}$ and $P_{\mathrm{refl}} = 80\,\mathrm{W}$. For the low frequency oscillations, the matching network is of good-matching, the average forward and reflected powers are $P_{\mathrm{fwd}} = 300\,\mathrm{W}$, and $P_{\mathrm{refl}} = 45\,\mathrm{W}$. The difference in value of P_{abs} between in Figs.3 and 4 is due to a sensitive dependence on the mismatch between the discharge and the power source, as will be seen in Section 4 for analysing the

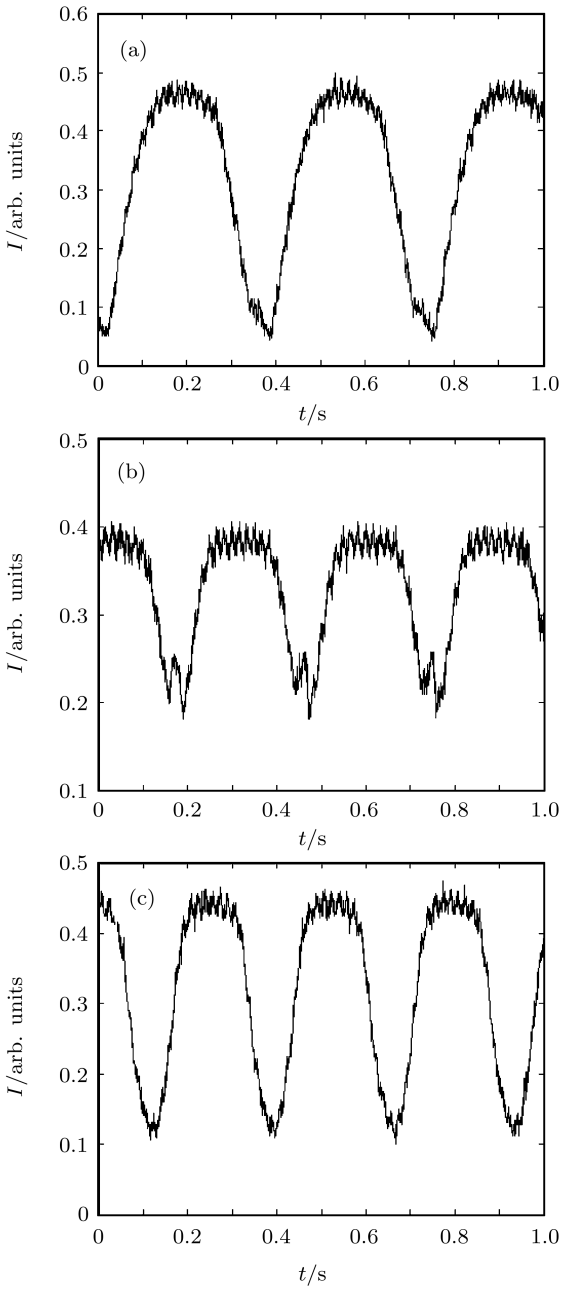


Fig.4. Time-varying optical emission I from the periphery, showing low frequency relaxation oscillations at $p = 100\,\mathrm{mT}$, (a) $f = 2.717\,\mathrm{Hz}$, $P_{\mathrm{abs}} = 325\,\mathrm{W}$; (b) $f = 3.484\,\mathrm{Hz}$, $P_{\mathrm{abs}} = 260\,\mathrm{W}$; (c) $f = 3.697\,\mathrm{Hz}$, $P_{\mathrm{abs}} = 176\,\mathrm{W}$, where the zero of I is not calibrated.

instability. We present in Table 1 ranges of the observed kilohertz and the hertz oscillations during a typical run in which the power is increased at a fixed pressure. When the absorbed power increases to 58 W, low frequency oscillations begin in the periphery ignited, in cases 8 to 11 low frequency oscillations occur in the periphery ignited. With the power increasing, the low frequency (several hertz) oscillation somewhat decreases. Low frequency oscillation depends on the

match extent between the discharge and the power source. In the first five cases of ascending $P_{\rm abs}$ (and also $P_{\rm fwd}$) but with slightly different matching conditions from each other, kilohertz oscillations are observed in the main discharge. Although not measured simultaneously, in similar cases oscillations with the same frequencies also occur in the slot. In cases 6–11, the peripheral plasma is ignited. The low frequency oscillation persists in the entire system due to the periphery that is ignited after the main discharge and the slot have been ignited, and then the main discharge plasma connects to the periphery by the slot, thereby with the periphery is ignited.

Table 1. Ranges of the observed high and low frequency oscillations.

case	$P_{\rm fw}$ /W	$P_{\rm refl}$ /W	$P_{\rm abs}$ /W	$V_{\rm rf}$(p-p) /V	I_M(p-p) /A	f kHz	f Hz	Visual inspection
1	60	45	15	151	3.29	38.2		slot mainly dark
2	80	60	20	169	3.68	35.2		plasma diffusion into slot
3	100	75	25	185	4.06	32.3		plasma diffusion into 1/4 slot
4	120	85	35	198	4.32	30.2		plasma diffusion further 1/2 slot
5	150	105	45	219	4.80	26.7		plasma diffusion further 3/4 slot
6	200	132	68	239	5.25	22.7		plasma diffusion into the entire slot
7	200	145	55	186	4.16	49.0		peripheral plasma ignited
8	250	192	58	188	4.26			low frequency oscillations begin in periphery
9	200	24	176	432	8.21		3.70	plasma diffusion further, grounded area increase
10	300	40	260	512	9.65		3.48	plasma diffusion further, grounded area increase
11	400	75	325	587	10.98		2.72	plasma diffusion further, peripheral plasma still ignited

3. Theory of high and low frequency relaxation oscillations

Ignition of slot plasma causes the main plasma voltage $V_{\rm p}$ to drop due to an increase of the grounded area seen by the main discharge. This will extinguish the slot discharge but may leave the main discharge ignited. However, the additional detuning of the match and the overall lowering of the circuit Q can also result in extinguishing the main discharge. Because the formation of a slot plasma results in the propagation of a surface wave with a significant phase shift and resistive decay, an electromagnetic analysis in the slot and periphery is relevant. However, this requires some simplifications as described below.

3.1. Electromagnetic analysis of the slot impedance

The impedance $Z_{\rm sl}$ of the slot seen from the main discharge is determined by an electromagnetic analysis. The slot plasma is driven at one end (its inner radius) by the rf voltage $V_{\rm p}$ of the main discharge plasma, with the top and bottom slot surfaces grounded through the quartz confinement rings. As shown in Refs.[2, 3], a transverse magnetic (TM) surface wave that propagates along the quartz-plasma interface is excited at the slot entrance. A rectangular coordinate model is used to determine the propagation and impedance characteristics, with x, y, and z corresponding respectively to the radial, axial and circumferential directions in a cylindrical geometry. The TM mode is independent of z. We assume open-circuit boundary conditions for the reflection of the wave at the slot exit. We determined the mode characteristics with Maxwell equations, of which the detailed discussion may be found in our previous paper.[5]

3.2. Interaction between the matching network and discharge

The kilohertz oscillation is found by increasing the source voltage V_T supplying rf power to the main discharge. As the voltage increases, the matching network elements C_M and L_M are adjusted to achieve a match of typically 75% in reflected power near the transition. For lower voltages, the main discharge appears steady and the slot appears to be dark, except for a 'finger' of plasma that diffuses about a half-

centimetre into the slot. When V_T is increased to over a certain threshold value, the kilohertz main discharge oscillation appears, and the slot lights up. Continue to increase power, then the low frequency oscillation will appear in the periphery. For the calculation we take the reflected power to be about 75% for a high frequency oscillation and the average reflected power to be 15% for a low frequency oscillation. The periphery usually remains dark during a high frequency oscillation, while a low frequency oscillation occurs in the periphery ignited, which will be assumed in the following calculation.

To determine the interaction between the source and the matching network with the whole system discharge, we solve the ladder-network shown in Fig.5, thereby obtaining the source voltage V_T as a function of the plasma voltage V_p in the main discharge. For a linear network, V_T is a linear function of V_p for any chosen slot density, but the slot and the periphery discharge nonlinearities significantly modify this property. The most important nonlinearities, which we retain in the analysis below, are the voltage-dependent main discharge sheath capacitances $C_a(V_a)$, $C_b(V_\mathrm{p})$ and $C_\mathrm{peri}(V_\mathrm{peri})$, where $V_a = V_D - V_\mathrm{p}$ is the voltage across the powered electrode sheath, V_p is the voltage across the grounded electrode sheath, V_peri is the voltage across the peripheral sheath, and $V_\mathrm{peri} = V_\mathrm{p} - I_\mathrm{sl}Z_\mathrm{sl}$. We use a collisional (constant mean free path) sheath model[4] to determine these capacitances

$$C_a = \kappa_\mathrm{cap}A_a/|V_a|^{3/5}; \quad C_b = k_\mathrm{cap}A_b/|V_b|^{3/5};$$

and

$$C_\mathrm{peri} = k_\mathrm{cap}A_\mathrm{peri}/|V_\mathrm{peri}|^{3/5} \tag{1}$$

where

$$\kappa_\mathrm{cap} = 1.25\varepsilon_0(en_\mathrm{s}u_\mathrm{B}/\varepsilon_0)^{2/5}(M/e\lambda_i)^{1/5} \tag{2}$$

with n_s being the density on the plasma-sheath edge. The sheath edge density (n_s) is taken to be $2.0 \times 10^9\,\mathrm{cm}^{-3}$, consistent with the value of V_bd determined from the breakdown model, and the electron temperature (T_e) taken to be 2 V. The matching network capacitance (C_M) was measured just prior to the transition to kilohertz oscillations to be about 2500 pF. We have chosen the discharge resistance (R_D) to be consistent with this measurement, thereby obtaining quite a reasonable value of 1.2 Ω, which keeps fixed in the calculation. The procedure for solving the ladder-network of Fig.5 is as follows: choosing a real V_p and a slot density n_sl, then $I_\mathrm{sl} = V_\mathrm{p}/(Z_\mathrm{sl} + 1/j\omega C_\mathrm{peri})$, C_b and C_peri are determined from expression (1) for the given V_p, V_peri, $I_b = j\omega C_b V_\mathrm{p}$ and $I_\mathrm{rf} = I_b + I_\mathrm{sl}$, and we obtain the equation $|V_a|\omega C_a(|V_a|) = |I_\mathrm{rf}|$, which can be solved to determine $|V_a|$ and C_a by using expression (1). When the peripheral plasma is ignited, the slot density n_sl is too large, thus Z_sl is too small and $V_\mathrm{peri} \approx V_\mathrm{p}$. In other words, C_peri can be considered to be connected to C_b in parallel, then $C_\mathrm{p} = C_b + C_\mathrm{peri} = \kappa_\mathrm{cap}(A_b + A_\mathrm{peri})/|V_\mathrm{p}|^{3/5} = \kappa_\mathrm{cap}A_\mathrm{ground}/|V_\mathrm{p}|^{3/5}$, where A_ground is a total grounded area. With the power increasing, A_ground is becoming large and the slot is ignited at high frequency oscillations. With the further increase of power, the ground area A_ground is much large, and the periphery is also ignited at a low frequency oscillation. Then $V_a = I_\mathrm{rf}/j\omega C_a$, $V_D = V_a + V_\mathrm{p}$, $V_\mathrm{rf} = V_D + I_\mathrm{rf}R_D$, $I_M = I_\mathrm{rf} + j\omega C_\mathrm{stray}V_\mathrm{rf}$, $V_M = j\omega L_M I_M + V_\mathrm{rf}$, $I_T = j\omega C_M V_M + I_M$, and, finally, $V_T = I_T R_T + V_M$.

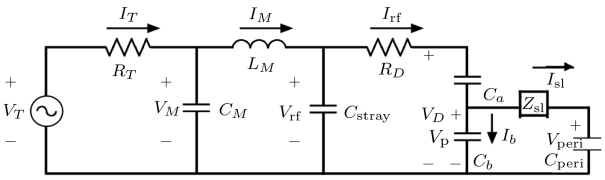


Fig.5. Circuit model of the rf power source, L-type matching network, main discharge region, dielectric slot region and peripheral region.

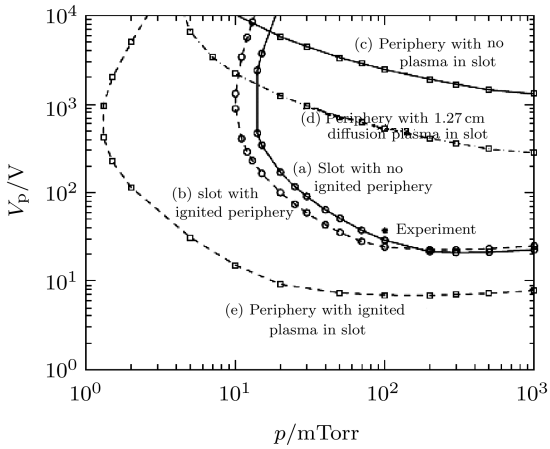


Fig.6. Maintenance curves for experimental condition: $f = 27.12\,\mathrm{MHz}$, $l = 2.54\,\mathrm{cm}$, $g = 0.635\,\mathrm{cm}$, $w = 3.8\,\mathrm{cm}$, and $w_\mathrm{per} = 5.1\,\mathrm{cm}$ with quartz dielectric confinement rings, where stars denote the measurements of peripheral plasma ignition. The slot plasma ignites at about 28 V (curve a). Once the slot ignites, the periphery also ignites, and periphery maintenance voltage is about 6 V with an ignited plasma in the slot (curve e).

Figure 7 shows $|V_T|$ versus V_p for eleven different slot densities, which we use below to provide a possible explanation for the kilohertz and the hertz oscillations that are observed experimentally. We discuss first the situation at the lowest density of $n_\mathrm{sl} \approx 1.0 \times 10^{13}\,\mathrm{m}^{-3}$ (curve a in Fig.7), where the slot plasma is essentially absent. For the chosen value of $|V_T|$, shown as the horizontal dashed line $V_{T_0} = 44.7\,\mathrm{V}$, there are three solutions for V_p, due to the high-Q resonance just below the breakdown voltage $V_\mathrm{bd} = 29\,\mathrm{V}$ of the slot. The largest solution for V_p corresponds to an operating point of the main discharge with the periphery ignited, the smallest V_p near zero corresponds to an extinguished main discharge, and the intermediate value is unstable. However, the matching elements L_M and C_M, and the source voltage V_{T_0} have been chosen such that the value of V_p at $|V_{T_0}|$ just exceeds the breakdown voltage of the slot, i.e. $V_\mathrm{bd} = 29\,\mathrm{V}$, with a 75% reflected power. In that case, the slot density increases on a fast (ionization) timescale to its maintenance value of $n_\mathrm{sl} \approx 2.0 \times 10^{15}\,\mathrm{m}^{-3}$ (curve f in Fig.7), determined from the condition of maintenance of plasma in the slot discussed in Ref.[2]. For this new slot density as shown in Fig.7, the only solution for V_p at the chosen $|V_T|$ is the extinguished main discharge state near $V_\mathrm{p} = 0$. Hence the voltages V_a and V_p decrease rapidly to zero. Since V_p now lies below V_bd, the slot plasma density decays. Referring to Fig.7, the main discharge remains extinguished until the slot density falls to a value just below $n_\mathrm{sl} \approx 6.8 \times 10^{14}\,\mathrm{m}^{-3}$ (curve d in Fig.7) when

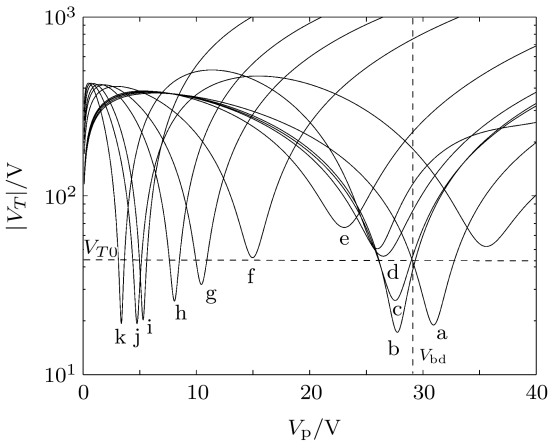


Fig.7. The source voltage $|V_T|$ versus sheath voltage V_p of main discharge grounded electrode for the whole processes of high and low frequency relaxation oscillations at different densities: 0.01 (a), 0.063 (b), 0.186 (c), 0.68 (d), 1.17 (e), 2.0 (f), 3.0 (g), 4.0 (h), 6.0 (i), 10 (j), 20 (k), in units of ($10^{15}\mathrm{m}^{-3}$) with variable capacitance C_p and variable impedance Z_sl at $p = 100\,\mathrm{mT}$.

the high-Q resonance dips (curves c and b in Fig.7) are below the horizontal dashed line V_{T_0}. At this point the main discharge re-ignites. The slot density continues to decay until $n_\mathrm{sl} \approx 1.0 \times 10^{13}\,\mathrm{m}^{-3}$ (curve a in Fig.7) when V_p again exceeds V_bd. At this point the slot re-ignites, and the cycle (a → f → a) repeats. This is reasonable explanation for high frequency relaxation oscillations in the main and the slot discharges.

For a low frequency relaxation oscillation in the peripheral discharge, when the absorbed power increases about 58 W, a low frequency oscillation begins. Specially, with about a 15% reflected power, $P_\mathrm{abs} = 176\,\mathrm{W}$, a low frequency(3.7 Hz) relaxation oscillation occurs in the periphery. The low frequency oscillation leads to an increase in grounded area when the periphery is ignited, thereby reducing the slot plasma potential (V_p) with respect to ground, and further reducing the potential to below the breakdown voltage ($V_\mathrm{p} < V_\mathrm{bd}$). The densities in the main discharge chamber and the slot increase, when the slot density $n_\mathrm{sl} \approx 6.0 \times 10^{15}\,\mathrm{m}^{-3}$ (curve i in Fig.7) in accordance with the case of $P_\mathrm{abs} \approx 176\,\mathrm{W}$. The high-Q resonance dips drop to just below $V_\mathrm{p} = 6\,\mathrm{V}$, and the discharges in the periphery and the slot are extinguished (the periphery maintenance voltage is about 6 V, as shown by curve e shown in Fig.6) and then V_p drops rapidly to zero, the main discharge is also extinguished. The slot and the periphery are restored to the plasma voltage, and the slot density decays. The process 'i → h → g → f → e → d → c → b → a' restarts, and the main discharge and the slot re-ignite. Once the slot is ignited, the periphery is also ignited, with absorbed power exceeding 55 W (shown in Table 1). V_p re-decreases; the density in the slot re-increases. When the density increases to $2.0 \times 10^{15}\,\mathrm{m}^{-3}$, V_p does not continue to decrease to zero because the absorbed power is 176 W in this case in which the reflected power is 15%, rather than $P_\mathrm{abs} = 15\,\mathrm{W}$, for the case in which the reflected power is 75%. The main discharge and the periphery are still ignited, so the slot density continues to increase. The slot and the periphery are ignited until $n_\mathrm{sl} \approx 6.0 \times 10^{15}\,\mathrm{m}^{-3}$. And then V_p decreases rapidly to zero, and the main discharge plasma is extinguished, thus the process 'a → b → c → d → e → f → g → h → i' is completed. The next step restarts the cycle 'i → a → i'. The absorbed power is 260 W, where the reflected power still maintains 15%(in case 10 in Table 1). A low frequency (3.48 Hz) relaxation oscillation appears in the periphery, and the density in slot continues to increase. When the slot

density $n_{\rm sl} \approx 1.0 \times 10^{16}\,{\rm m}^{-3}$ (curve j in Fig.7) in accordance with the case of $P_{\rm abs} \approx 260\,{\rm W}$. The high-Q resonance dips drop at $V_{\rm p} \approx 4.9\,{\rm V}$, due to the hysteresis behaviour below the periphery-discharge maintaining voltage 6 V. The discharges of periphery and slot are extinguished, and the main discharge is also extinguished when $V_{\rm p}$ decreases to zero. Thus the process 'a → b → c → d → e → f → g → h → i → j' is completed, and the cycle 'j → a → j' repeats. With the same analysis, another low frequency (2.72 Hz) oscillation is present in the periphery in case 11 of Table 1, and a new cycle 'k → a → k' occurs as shown in Fig.7.

From Fig.7, we can see that each cycle of low frequency oscillations (e.g. 'i → a →i', 'j → a →j' and 'k → a →k') has a longer period than that of high frequency oscillations (e.g. 'f → a → f'). we also see that the period of 'k → a → k' is longer than one of 'j → a → j' or 'i → a → i', due to $f_k < f_j < f_i$ (2.717 Hz $<$ 3.484 Hz $<$ 3.697 Hz). We can explain the low frequency relaxation oscillation phenomena successfully. We obtain an oscillation frequency from the following derivation:

$$V{\rm d}n_{\rm e}/{\rm d}t = K_{\rm iz} n_g n_{\rm e} V - n_{\rm s} u_{\rm B} 2A.$$

where $V = Ad$, $n_{\rm s} = h_l n_{\rm e}$, $h_l = 0.86(3 + l/2\lambda_i)^{-1/2}$, and $\lambda_i = 1/33p$, with λ_i being in metres, p in mTorr, A being plate area, d plasma thickness, $n_{\rm s}$ edge density, n_e central density, h_l Godyak factor.[3] For the decay time, drop the $K_{\rm iz}$ term, then we will have

$$V{\rm d}n_e/{\rm d}t = -n_s u_{\rm B} 2A, \quad \text{and} \quad {\rm d}{\rm d}n_e/{\rm d}t = -2h_l n_e u_{\rm B},$$

where $u_{\rm B} = (eT_e/M)^{1/2}$ is the Bohm speed. From the above, we have

$$\int_0^t {\rm d}t = -d/2h_l u_{\rm B} \int_{n_0}^{n_{\rm e}} {\rm d}n_{\rm e}/n_{\rm e}, \quad n_{\rm e} = n_0 {\rm e}^{-2h_l u_{\rm B} t/d},$$

thereby obtaining the decay time:

$$t = d/2h_l u_{\rm B} \ln(n_0/n_e) = \tau_{\rm sl} \ln(n_1/n_2).$$

We have used a simple exponential model for the high frequency oscillation in slot plasma density decay, with the timescale $\tau_{\rm SR}$ determined from diffusion theory to be

$$\tau_{\rm sl} = g/2h_{\rm gsl} u_{\rm Bsl}, \tag{3}$$

with

$$h_{\rm gsl} = 0.86/(3 + g/\lambda_i)^{1/2}, \tag{4}$$

the edge-to-centre density ratio in the slot. Using a reasonable slot temperature during the decay, i.e. $T_{\rm esl} = 1\,{\rm V}$, we obtain the decay time $\tau_{\rm sl} = 8.8\,\mu{\rm s}$, due to the signal pulse rising rapidly during the on-time. With a density decay from $n_1 \simeq 2 \times 10^{15}\,{\rm m}^{-3}$ to $n_2 \simeq 1.86 \times 10^{14}\,{\rm m}^{-3}$, $f = 1/\tau_{\rm sl} \ln(n_1/n_2) \simeq 46\,{\rm kHz}$. For the low frequency oscillation in slot plasma density decay, with the timescale $\tau_{\rm SR}$ determined from diffusion theory to be $\tau_{\rm sl} = l/2h_l u_{\rm B}$, where $h_l = 0.86(3 + l/2\lambda_i)^{-1/2}$. So the estimate decay time $\tau_{\rm sl} = 48.36\,{\rm ms}$, with a density decay from $n_1 \simeq 2.0 \times 10^{16}\,{\rm m}^{-3}$ to $n_2 \simeq 1.0 \times 10^{13}\,{\rm m}^{-3}$, $f = 1/\tau_{\rm sl} \ln(n_1/n_2) \simeq 2.7\,{\rm Hz}$.

4. Conclusions and further discussion

The kilohertz oscillations observed in the central plasma and in the slot connected to the peripheral chamber, at voltages below which the peripheral plasma ignites, are essentially understood as an instability induced by the increased resistance and capacitance of the discharge when the slot plasma ignites. A particular tuning of the matching network that we have investigated, both experimentally and theoretically, indicates that the transient ignition of the slot plasma increases the capacitance of the plasma to ground and lowers the system Q in such a way that the overall equilibrium is lost. This causes the voltage across the discharge to drop dramatically, thereby leading the electron temperature to decrease. The main discharge density correspondingly decays but at a slower rate, until the faster decay of the slot plasma density re-ignites the discharge, repeating the scenario. The oscillation frequency as well as the shapes of the light emission signal and plasma density, obtained from the model, agree reasonably well with the corresponding experimental observations.

We have explained high frequency relaxation oscillations by using an electromagnetic model of the slot impedance combined with the circuit analysis of system including the match network in the previous study. For low frequency relaxation oscillations, although we described some experimental phenomena of low frequency oscillations in the previous papers,[5–8] we did not further discuss the origin of low frequency oscillations. In this paper we develop a model in which various capacitances in the slot and the periphery varying with increase of absorbed power are considered and the grounded area A_b increases. The capacitance C_b increases with the increase of the grounded area A_b when the periphery is ignited, which is equiv-

alent to a parallel connection of a variable peripheral capacitance $C_{\rm peri}$ to C_b. The relaxation oscillations, which depend nonlinearly on the two states of the discharge, have some similarities to those we have previously studied in electronegative discharges.[9,10] In that case the timescales of the electrons and negative ions, which controlled the frequency and the amplitude of the instability were different, the slowest timescale for decay of the negative ion density essentially controlled the frequency. For the configuration under study here, there is also a difference in timescale, on the assumption that the fast ionization time controls the ignition of the slot plasma and the slower timescale for plasma decay in the slot controls the oscillation frequency. In both situations, the matching network dynamics has been found to play an important role in the instability dynamics.

References

[1] Tsai W, Mueller G, Lindquist R, Frazier B and Vahedi V 1996 *J. Vac. Sci. Technol.* B **14** 3276

[2] Lieberman M A, Lichtenberg A J, Kim S, Gudmundsson J T, Keil D L and Kim J 2006 *Plasma Sources Sci. Technol.* **15** 276

[3] Lieberman M A, Booth J P, Chabert P, Rax J M and Turner M M 2002 *Plasma Sources Sci. Technol.* **11** 283

[4] Lieberman M A and Lichtenberg A J 2005 *Principles of Plasma Discharges and Materials Processing* (New York: Wiley)

[5] Kim S, Zhou Z, Lieberman M A and Lichtenberg A J 2006 *J. Appl. Phys.* **100** 103302

[6] Kim S, Lieberman M A, Lichtenberg A J and Gudmundsson J T 2006 *J. Vac. Sci. Technol.* A **24** 2025

[7] Zhou Z W, Lieberman M A and Kim S 2006 *Chin. Phys. Lett.* **23** 2251

[8] Zhou Z W, Lieberman M A and Kim S 2007 *Chin. Phys.* **16** 758

[9] Chabert P, Lichtenberg A J, Lieberman M A and Marakhtanov A M 2001 *Plasma Sources Sci. Technol.* **10** 478

[10] Chabert P, Lichtenberg A J, Lieberman M A and Marakhtanov A M 2003 *J. Appl. Phys.* **94** 831